Title

East Asian hydroclimate modulated by the position of the westerlies during Termination I

Journal

Science, 362(6414)

ISSN

0036-8075

Authors

Zhang, Hongbin
Griffiths, Michael L
Chiang, John CH
et al.

Publication Date

2018-11-02

DOI

10.1126/science.aat9393

Peer reviewed

East Asian hydroclimate modulated by the position of the westerlies during Termination I

Hongbin Zhang[1,2], Michael L. Griffiths[3]*, John C. H. Chiang[4], Wenwen Kong[4], Shitou Wu[5,6], Alyssa Atwood[4,7], Junhua Huang[2], Hai Cheng[8,9], Youfeng Ning[8], Shucheng Xie[1,10]*

[1] State Key Laboratory of Biogeology and Environmental Geology, China University of Geosciences, Wuhan, 430074, China. [2] State Key Laboratory of Geological Processes and Mineral Resources, China University of Geosciences, Wuhan, 430074, China. [3] Department of Environmental Science, William Paterson University, Wayne, NJ 07470, USA. [4] Department of Geography and Berkeley Atmospheric Sciences Center, University of California, Berkeley, CA 94720, USA. [5] Department of Geochemistry, Faculty of Geoscience and Geography, Georg-August University Goettingen, Goettingen 37077, Germany. [6] Institute of Geology and Geophysics, Chinese Academy of Sciences, Beijing, 100029, China. [7] School of Earth and Atmospheric Sciences, Georgia Institute of Technology, Atlanta, GA 30332, USA. [8] Institute of Global Environmental Change, Xi'an Jiaotong University, Xi'an, 710049, China. [9] Department of Earth Science, University of Minnesota, Minneapolis, MN 55455, USA. [10]Department of Geography, School of Earth Sciences, China University of Geosciences, Wuhan, 430074, China.

*Corresponding author. Email: xiecug@163.com (S.X.); griffithsm@wpunj.edu (M.L.G.)

Abstract

Speleothem oxygen isotope records have revolutionized our understanding of the paleo East Asian monsoon, yet there is fundamental disagreement on what they represent in terms of the hydroclimate changes. We report a multiproxy speleothem record of monsoon evolution during the last deglaciation from the middle Yangtze region, which indicates a wetter central eastern China during North Atlantic cooling episodes, despite the oxygen isotopic record suggesting a weaker monsoon. We show that this apparent contradiction can be resolved if the changes are interpreted as a lengthening of the Meiyu rains and shortened post-Meiyu stage, in accordance with a recent hypothesis. Model simulations support this interpretation and further reveal the role of the westerlies in communicating the North Atlantic influence to the East Asian climate.

Introduction

Speleothem oxygen isotope records ($\delta^{18}O_c$) from China have revealed the most detailed insights into past Asian summer monsoon variability of any climate proxy to date (*1*–*3*). A recent study by Cheng *et al*. (*3*) was the first to extend the Chinese cave records back to the dating limits of uranium-thorium (~640,000 years), providing critical new insight into the nature and cause(s) of Asian summer monsoon variability, and importantly, its connection with glacial terminations. Moreover, numerous studies have also shown a strong link between $\delta^{18}O_c$ and millennial-scale perturbations of the last glacial and deglaciation, such as Heinrich events, characterized by large freshwater discharges into the North Atlantic that corresponded with higher

$\delta^{18}O_c$ in Chinese speleothems, interpreted as a weakening of the monsoon (*1*, *4*).

However, we still lack critical understanding of what exactly $\delta^{18}O_c$ represents in terms of large-scale shifts in Asian summer monsoon circulation, and more "local-scale" changes in precipitation. The prevailing literature presents a number of competing interpretations. The traditional interpretation links $\delta^{18}O_c$ as a proxy for East Asian summer monsoon (EASM) "strength" or "intensity," defined in terms of large seasonal differences in precipitation oxygen isotopes ($\delta^{18}O_p$), where higher EASM rainfall corresponds with more depleted $\delta^{18}O_c$ (*1*, *2*). By contrast, others have interpreted $\delta^{18}O_c$ as reflecting changes in the fraction of water vapor rained out along the moisture trajectory between tropical sources and the cave site (*4*, *5*); subsequent isotope-enabled general circulation model (GCM) simulations support this latter interpretation, although they emphasized the "upstream depletion" rather than "local depletion" at the cave site (*6*, *7*). More recent interpretations attempt to reconcile these two end-members, calling for $\delta^{18}O_c$ to represent EASM intensity via changes in the strength of the southerly monsoon flow and associated heterogeneous expression of EASM rainfall, with lower $\delta^{18}O_c$ implying higher upstream rainout integrated between different moisture sources en route to the cave sites, but not local rainfall (*3*, *8*).

The second challenge arises from consideration of the observed seasonal evolution of the EASM (*9*, *10*). Unlike other monsoons that have only one rainfall stage, the seasonal rainfall evolution over East Asia undergoes a number of quasi-stationary intraseasonal stages with abrupt transitions in between (*10*) (Fig. 1A). During spring, persistent rainfall in southern China is followed by substantial convection over the South China Sea during the pre-Meiyu stage in mid-May. By mid-June, the Meiyu begins and rainfall shifts to central China, and around mid-July, the rain band shifts again to be located over northeast China, marking the onset of the midsummer stage, which terminates around mid-August. Moreover, dynamical arguments link these stages to the configuration of the westerlies impinging on the Tibetan Plateau; as the peak westerlies migrate from the south to the north of the Plateau and off it, the downstream circulation changes and thus determines the various intraseasonal stages (*11*–*13*). In other words, the EASM undergoes a complex spatiotemporal evolution, and so it is unclear what "intensity" means in this context.

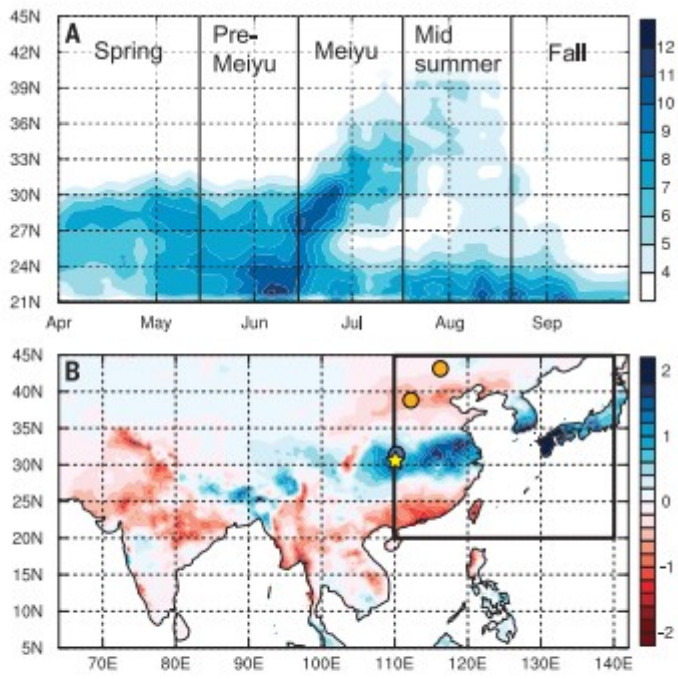

Fig. 1. Cave location and climatology of East Asia. (**A**) Hovmöller diagram of the precipitation climatology (unit: mm/day) over eastern China (110° to 120°E). Approximate timings of the various stages are shown. (**B**) Spatial pattern of the dominant tripole mode of interannual variability in rainfall over East Asia. Chiang *et al.* (*27*) showed the first empirical orthogonal function (EOF) and the normalized first principle component (PC1) of July-August mean precipitation over East Asia (110° to 145°E, 20° to 45°N) [area indicated by the black box in (B); see figures 1, b and c, of Chiang *et al.* (*27*)]. Here we show the regression of the PC1 of Chiang *et al.* (*27*) onto the July-August rainfall across Asia. We use the APHRODITE dataset spanning 1951 to 2007. Units in (B) are mm/day per standard deviation. The yellow star denotes Haozhu Cave (this study), the blue circle shows Dajiuhu peatland (*23*), and orange circles represent Gonghai Lake (*24*) and Dali Lake (*25*) as plotted in Fig. 2.

To address these uncertainties, here we present a new multiproxy record of EASM variability from two absolute-dated speleothems from central eastern China (*14*), which extends through the last deglaciation [~10 to 21 thousand years (ka) before the present (B.P.)]. The two specimens (HZZ11 and HZZ27) were recovered from Haozhu Cave (109°59′ E, 30°41′ N, 1017 m), located in the Hubei Province of central China (Fig. 1B). We examined both $\delta^{18}O_c$ and trace elements (Mg^{2+}, Sr^{2+}, Ba^{2+}) in two speleothems to help deconvolve large-scale EASM circulation [inferred from $\delta^{18}O_c$ (*3*, *8*)] from local hydrology (inferred from the trace elements) during Termination I (supplementary materials). The isotopic and elemental profiles were anchored by 22 U-Th dates by using linear interpolation between each successive date and further refined by aligning major $\delta^{18}O_c$ excursions within their respective age uncertainties (fig. S4). Although only representing a minor contribution to speleothem paleoclimate studies (relative to $\delta^{18}O_c$), research has increasingly shown that trace elements can faithfully record environmental (particularly hydrological) changes operating in and between the cave interior and soil zone (*15*). Hence, these elemental ratios reflect more local hydrological changes happening at the site of deposition (*16*, *17*), and thus when paired with oxygen isotopes, can add valuable information to proxy interpretations.

Results show that the HZZ11 and HZZ27 $\delta^{18}O_c$ time series largely parallel those from other distal cave sites in China and India, showing enriched $\delta^{18}O_c$ values during North Atlantic cooling events [i.e., Heinrich event 1 (H1) and the Younger Dryas (YD)] and more depleted $\delta^{18}O_c$ values during the Bølling-Allerød (B-A) interstadial (Fig. 2A and fig. S2). In addition, these millennial-scale $\delta^{18}O_c$ fluctuations are also consistent with a record of terrigenous sediment flux (*18*) (Fig. 2B)—a proxy for the Indian summer monsoon—into the Arabian Sea. Recent hydroclimate reconstructions of the tropical Indian Ocean, combined with model simulations, demonstrate that a weakened Indian monsoon circulation during North Atlantic stadials was likely caused by a reorganization of the Hadley circulation with a southward shift of the ascending branch—the intertropical convergence zone (ITCZ) (*19*). Taken together, these records are consistent with the interpretation that North Atlantic stadial events led to an overall weakening of the Asian summer monsoon via declines in hemispheric surface temperatures and subsequent meridional displacements of the ITCZ (*1*, *8*, *18*, *19*).

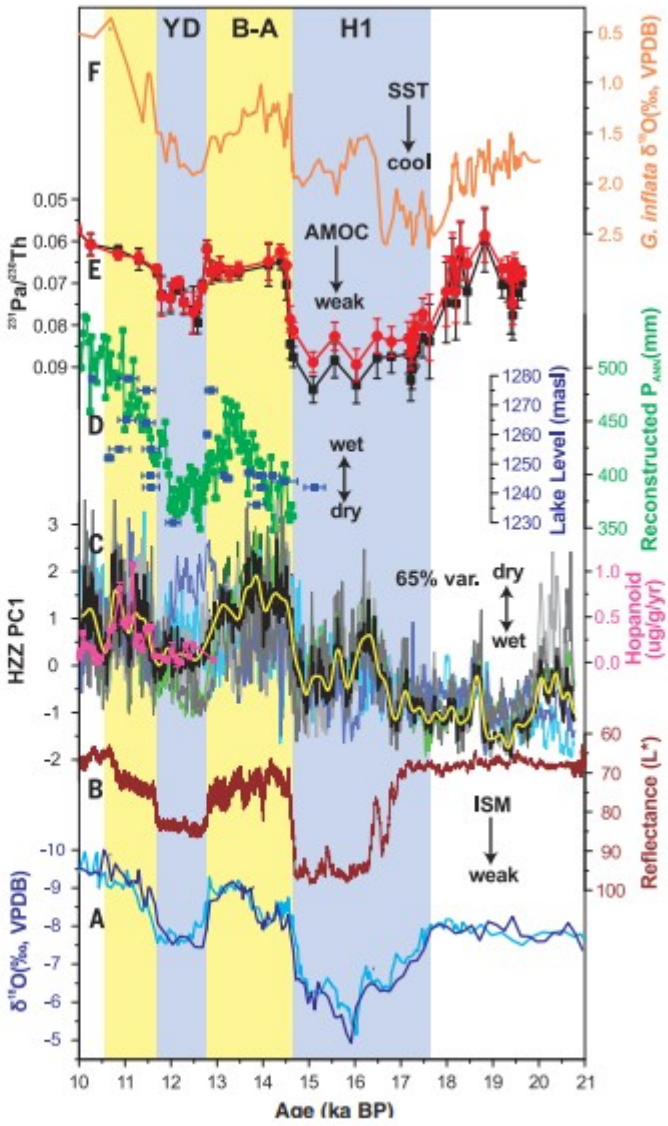

Fig. 2. Central China hydroclimate and high northern latitude teleconnections during the last deglaciation. (**A**) $\delta^{18}O$ records of HZZ11 and HZZ27 (*14*). VPDB, Vienna Pee Dee belemnite. (**B**) Arabian Sea sediment total reflectance (L*), a proxy for Indian summer monsoon (ISM) strength (*18*). (**C**) Leading PC (HZZ PC1; black curve) of HZZ11 and HZZ27 Mg/Ca, Sr/Ca, and Ba/Ca records and hopanoid flux (pink curve), a proxy for water-table depth from nearby Dajiuhu peatland (*23*). Overlapped thin lines show the standardized Sr/Ca, Mg/Ca, and Ba/Ca records. Yellow line shows HZZ PC1 smoothed with a 100-year loess filter. (**D**) Reconstructed annual precipitation (green) and lake level (blue) in North China from Gonghai Lake (*24*) and Dali Lake (*25*), respectively. (**E** and **F**) North Atlantic sediment core GGC5 $^{231}Pa/^{230}Th$ (proxy for AMOC) and planktonic foraminifera $\delta^{18}O$ [proxy for sea surface temperature (SST)] (*22*).

Our speleothem trace-element results, however, offer a more complex story. Indeed, analyses of Sr-Mg-Ba/Ca (hereafter X/Ca) ratios in both speleothems reveal that during H1 and YD, X/Ca values decreased significantly, whereas during the B-A interstadial, values abruptly increased (Fig. 2C and fig. S6). Significant correlations amongst the various trace element–to–calcium ratios (fig. S7) suggest that similar processes controlled their variability, which can be summarized as follows: Higher values indicate overall drier conditions when reduced infiltration within the karst fracture network favors CO_2 degassing and prior calcite precipitation (PCP) in the epikarst, leaving the cave drip-water, and hence speleothems, enriched in the trace elements relative to calcium; the opposite occurs during wetter periods (*15*, *20*). However, drier conditions may have prolonged water-rock interaction (WRI) in the aquifer, which would have favored selective leaching of Mg and Sr from the dolomite host rock (*21*), causing enrichment in Mg and Sr (fig. S8)

(see supplementary text for more details). Nonetheless, whichever mechanism dominated, it is apparent that drier (wetter) intervals would have favored higher (lower) X/Ca values in HZZ11 and HZZ27 during the deglaciation.

To effectively combine the X/Ca records for both speleothems into one composite hydroclimate record, we calculated the leading principal component ("HZZ PC1") on the six trace-element time series, where lower values indicate wetter conditions and higher values, drier conditions. Examination of HZZ PC1 reveals that the region became wetter during the H1 and YD stadials (Fig. 2C), when the abrupt input of fresh water to the North Atlantic led to declines in the Atlantic Meridional Overturning Circulation (AMOC) (Fig. 2E) and resultant lowering of SSTs (*22*) (Fig. 2F). This finding is compelling because it shows that, despite a weakened Asian summer monsoon (Fig. 2, A and B), central China was in fact wetter during these stadial events, while similar to southern Asia, northern China was drier (*8*, *23*–*25*) (Fig. 2, C and D). The HZZ PC1 results also suggest that central eastern China was wetter during the Last Glacial Maximum (LGM; ~19 ka B.P.) and experienced an overall drying trend until the early Holocene; this trend is supported by speleothem $\delta^{13}C$ and initial uranium isotope ratios from the same specimens, which we interpret to reflect local hydrology (figs. S5 and S6 and supplementary text).

At face value, these phase relationships in the EASM region suggest antiphasing of rainfall between central and northeastern China. Liu *et al*. (*8*) first noted an inhomogeneity in the simulated East Asian rainfall response to climate forcing over the last 21,000 years, specifically tying a negative $\delta^{18}O_p$ signal over China with enhanced monsoon rainfall restricted to northeastern China. However, the antiphased relationship has a more direct analog to the observed modern interannual variability. The dominant mode of summer rainfall variability over East Asia is characterized by a meridional "tripole" pattern of precipitation, with increased rainfall over northeastern and southeastern China and decreased rainfall over central eastern China and Japan (*12*, *26*, *27*) (Fig. 1B). Moreover, this pattern is also known to covary with strengthened Indian summer monsoon rainfall in South Asia (*28*). Hence, this modern-day analog appears relevant to understanding the East Asian rainfall response during the H1 and YD events. However, the question remains why East Asian climate responds this way during North Atlantic stadials. To help answer this, we analyzed a freshwater "hosing" simulation using the Community Earth System Model (CESM) version 1.0.5 of the National Center for Atmospheric Research (NCAR). Specifically, the control run was perturbed with 1 Sv (1 Sv = 10^6 m^3 s^{-1}) of freshwater injection into the North Atlantic to simulate a rapid shutdown of the AMOC akin to H1 and the YD.

Our model results are consistent with HZZ PC1 and other proxy records (*8*, *23*–*25*), which show an increase in summer rainfall in central eastern China and a decrease in northern China during stadial events of the deglaciation (Fig. 3A). A recent hypothesis—the "jet transition hypothesis" (*10*)—argues that rainfall changes over East Asia arise through changes in the transition timing and duration of the EASM intraseasonal stages (i.e., spring, pre-Meiyu, Meiyu, and midsummer), which are in turn tied to the south-north displacement of the westerlies relative to the Tibetan Plateau. In particular, the tripole pattern of the interannual variability arises from variation in the termination date of Meiyu; an earlier termination shortens the Meiyu stage and lengthens the midsummer stage, leading to less rain over central eastern China and more over northeastern China. A paleoclimate modeling study found support for this hypothesis in precession-driven EASM changes during the Holocene (*29*). More precisely, the simulated decreased pole-equator temperature gradient during the early Holocene resulted in an earlier northward positioning of the westerlies relative to the Tibetan Plateau, leading to an earlier termination of the Meiyu stage and prolonged midsummer stage. The hypothesis also provided a simple and physically consistent explanation for the "the asynchronous Holocene optimum" (*30*), where the Holocene peak in East Asian hydroclimate was observed to occur earlier for northeastern China but later for central and southeastern China.

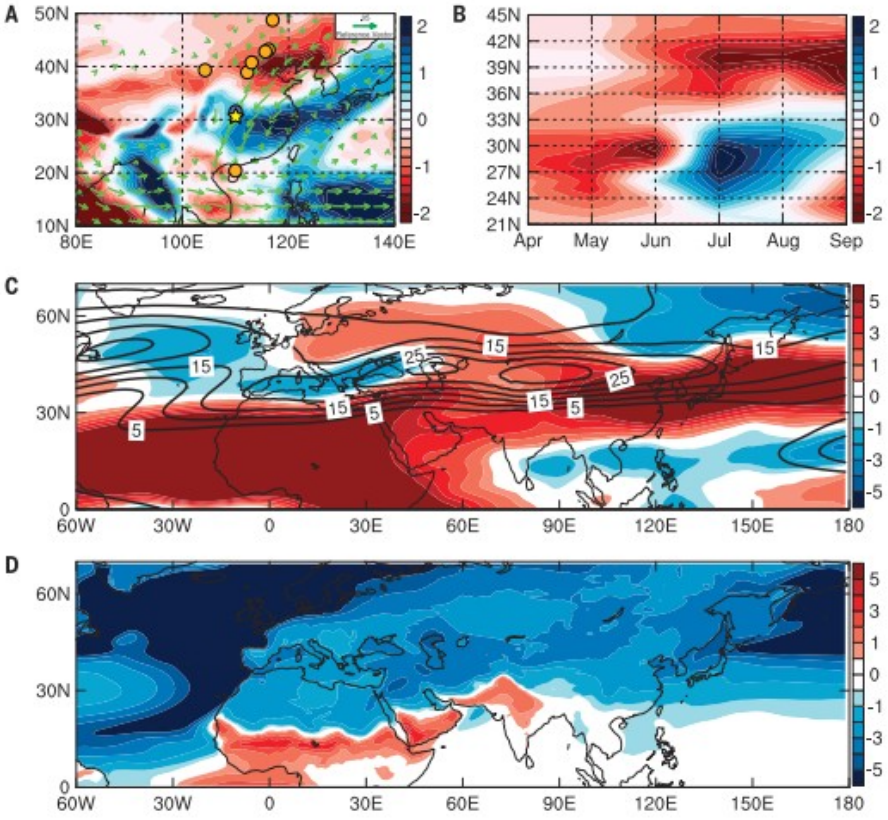

Fig. 3. CESM 1.0.5 simulated precipitation and Asian westerlies anomalies between 1-Sv hosing experiment and control simulation. (**A**) July-August rainfall anomalies in East Asia (shading; unit: mm/day) superimposed with moisture flux anomalies at 850 mb (vectors; unit: kg/kg-m/s). The yellow star and blue circle show sites [Haozhu cave (star, this study) and Dajiuhu peatland (circle, (23)] indicating wet conditions during H1 and/or YD, and orange circles show sites indicating dry conditions during H1 and/or YD (see fig. S1 for list of sites). (**B**) Hovmöller diagram of rainfall anomalies zonally averaged between 110° and 120°E (unit: mm/day). This shows the increase in rainfall over central eastern China in July-August and decreased rainfall to the north. (**C**) July-August zonal wind at 200 mb from the control run (contour; interval 5 m/s) and anomalies from the 1-Sv hosing run (shading), showing the equatorward displacement of the jet in the hosing simulation. (**D**) July-August air-temperature anomalies at 2 m above ground (unit: K). One hundred years climatology of the control run and 80 years climatology of the hosing run after spin-up were used to generate the anomalies.

We invoke a similar mechanism to explain the observed antiphasing of hydroclimate across China during H1 and the YD. Indeed, the simulated seasonal evolution of rainfall over central eastern China shows the distinct characteristics of a longer Meiyu and shortened midsummer stage (Fig. 3B), with increased rainfall over central eastern China and reduced rainfall over northeastern China during July and August (note that climatological midsummer stage is between mid-July through end of August). Moreover, the westerlies during July and August were displaced southward (Fig. 3C), consistent with a delayed northward migration. This delayed migration occurs because of the colder conditions in the northern extratropics (Fig. 3D) as a result of the AMOC slowdown, which increases the equator-to-pole temperature gradient. Thus, the jet transition hypothesis (*10*) provides a simple and consistent explanation for both the observed antiphasing of rainfall between north and central eastern China and the simulated large-scale response of the East Asian hydroclimate to AMOC slowdown representative of the YD and H1. It is also possible that this hypothesis, particularly as it relates to shifts in the equator-to-pole temperature gradient, can explain the wetter conditions in central eastern China during the LGM, although this will need to be further tested with additional proxy records and model simulations.

Critically, our results can be combined with previous isotope-enabled model results to provide a more comprehensive view of the paleo EASM system. In particular, Liu *et al*. (*8*) find model evidence that speleothem $\delta^{18}O_c$ reflects changes to the strength of the southerly monsoonal flow over East Asia—specifically, heavier $\delta^{18}O_c$ values indicate reduced monsoonal flow that translates to reduced rainfall over northeastern China. Our simulations do indeed show weaker southerlies and reduced northeastern China moisture transport with a reduced AMOC (Fig. 3A and fig. S9), thus providing a link between circulation changes that influence $\delta^{18}O_p$ and rainfall variability inferred in our simulations. Indeed, as elaborated in Chiang *et al*. (*10*), the meridional jet position is seen to limit the northward extent of the southerly monsoon flow penetrating into East Asia (figs. S9 and S10), with the northward migration of the jet allowing for a more northward penetration of the monsoon flow. This view nicely integrates the jet transition hypothesis with the hypothesis provided by Liu *et al*. (*8*) (i.e., the “moisture transport hypothesis”) and provides the link between our results and $\delta^{18}O_c$ in lieu of our own isotope-enabled model simulation.

The results of this study support the strong teleconnections between East Asia and the North Atlantic during the deglaciation, but notably, lend credence to the jet transition hypothesis (*10*). Our results also suggest that a stronger meridional temperature gradient [i.e., during stadial events (Fig. 3D)] and resultant southward-shifted and strengthened westerlies (Fig. 3C and fig. S10) can lead to increased convection and uplift of moisture on the leeward side of the Tibetan Plateau during the summer months in central

eastern China. This pattern, invoking wetter conditions to the south but drier conditions to the north, calls for a reevaluation of the regional heterogeneity of East Asian hydroclimate during abrupt climate perturbations of the last glacial cycle (*8*). These findings highlight the potential for abrupt and prolonged redistributions of moisture across East Asia under varying boundary conditions, which has important implications for future projections of rainfall in this densely populated region, particularly in light of the “north drought–south flood” pattern that has persisted in China since the 1970s (*31*).

REFERENCES AND NOTES

1. Y. J. Wang et al., Science 294, 2345–2348 (2001). 2. H. Cheng et al., Science 326, 248–252 (2009). 3. H. Cheng et al., Nature 534, 640–646 (2016). 4. D. Yuan et al., Science 304, 575–578 (2004). 5. C. Y. Hu et al., Earth Planet. Sci. Lett. 266, 221–232 (2008). 6. A. LeGrande, G. Schmidt, Clim. Past 5, 441–455 (2009). 7. F. S. R. Pausata, D. S. Battisti, K. H. Nisancioglu, C. M. Bitz, Nat. Geosci. 4, 474–480 (2011). 8. Z. Y. Liu et al., Quat. Sci. Rev. 83, 115–128 (2014). 9. Y. Ding, J. C. L. Chan, Meteorol. Atmos. Phys. 89, 117–142 (2005). 10. J. C. Chiang et al., Quat. Sci. Rev. 108, 111–129 (2015). 11. T. C. Yeh, S. J. Dao, M. T. Li, [The abrupt change of circulation over the Northern Hemisphere during June and October] in The Atmosphere and the Sea in motion, B. B., Ed. (Rockefeller Inst. Press, New York, 1959), pp. 249-267. 12. H. H. Hsu, X. Liu, Geophys. Res. Lett. 30, 1182–1200 (2003). 13. P. Molnar, W. R. Boos, D. S. Battisti, Annu. Rev. Earth Planet. Sci. 38, 77–102 (2010). 14. H. Zhang et al., Earth Planet. Sci. Lett. 453, 243–251 (2016). 15. I. J. Fairchild, P. C. Treble, Quat. Sci. Rev. 28, 449–468 (2009). 16. Y. H. Liu et al., Nat. Geosci. 6, 117–120 (2013). 17. M. L. Griffiths et al., Nat. Commun. 7, 11719 (2016). 18. G. Deplazes et al., Nat. Geosci. 6, 213–217 (2013). 19. M. Mohtadi et al., Nature 509, 76–80 (2014). 20. K. R. Johnson, C. Y. Hu, N. S. Belshaw, G. M. Henderson, Earth Planet. Sci. Lett. 244, 394–407 (2006). 21. I. J. Fairchild et al., Chem. Geol. 166, 255–269 (2000). 22. J. F. McManus, R. Francois, J. M. Gherardi, L. D. Keigwin, S. Brown-Leger, Nature 428, 834–837 (2004). 23. S. C. Xie et al., Geology 41, 827–830 (2013). 24. F. Chen et al., Sci. Rep. 5, 11186 (2015). 25. Y. Goldsmith et al., Proc. Natl. Acad. Sci. U.S.A. 114, 1817–1821 (2017). 26. H. H. Hsu, S. M. Lin, J. Clim. 20, 4443–4458 (2007). 27. J. C. H. Chiang, L. M. Swenson, W. Kong, Geophys. Res. Lett. 44, 3788–3795 (2017). 28. J. A. Day, I. Fung, C. Risi, J. Clim. 28, 4330–4356 (2015). 29. W. Kong, L. M. Swenson, J. C. Chiang, J. Clim. 30, 3343–3365 (2017). 30. Z. An et al., Quat. Sci. Rev. 19, 743–762 (2000). 31. R. Yu, B. Wang, T. Zhou, Geophys. Res. Lett. 31, 217–244 (2004).

ACKNOWLEDGMENTS

We gratefully acknowledge two anonymous reviewers for their constructive comments and C. Hu for the personal communication about cave monitoring work in Heshang Cave. We thank D. S. Battisti and C. M. Bitz for their assistance in developing the model simulations. Funding: This work was supported by the Key R&D Project of Ministry of Science and Technology (grant no. 2016YFA0601100), the Chinese National Natural Science Foundation (grants 41330103 and 41773135), the 111 Program (National Bureau for Foreign Experts and Ministry of Education of China; grant B08030), and the U.S. National Science Foundation (grant AGS-1405479). Author contributions: H.Z., M.L.G., S.X., and J.H. designed the project. H.Z. and J.H. performed the fieldwork and sampling. H.Z., H.C., and Y.N. carried out the uranium-thorium dating. H.Z. and J.H. contributed to the oxygen-isotope measurements. S.W. carried out the trace element measurements. J.C.H.C. and W.K. analyzed the modeling simulations, which were conducted by A.A. H.Z., M.L.G., S.X., J.C.H.C., and W.K. wrote the manuscript with contributions from other authors. All authors discussed the results and implications and commented on the manuscript at all stages. Competing interests: All authors declare no competing interests. Data and materials availability: All data reported in this paper are available in the supplementary materials.